

# Supporting Information

## Semiconducting polymer nanoporous thin films as a tool to regulate intracellular ROS balance in endothelial cells

*Miryam Criado-Gonzalez,<sup>1\*</sup> Luca Bondi,<sup>2</sup> Camilla Marzuoli,<sup>3,4</sup> Edgar Gutierrez-Fernandez,<sup>1,5</sup>*

*Gabriele Tullii,<sup>3</sup> Carlotta Ronchi,<sup>3</sup> Elena Gabirondo,<sup>1</sup> Haritz Sardon,<sup>1</sup> Stefania Rapino,<sup>6</sup> Marco*

*Malferrari,<sup>6</sup> Tobias Cramer,<sup>2</sup> Maria Rosa Antognazza,<sup>3</sup> and David Mecerreyes<sup>1,7\*</sup>*

<sup>1</sup> POLYMAT, University of the Basque Country UPV/EHU, Paseo Manuel de Lardizabal 3, 20018 Donostia-San Sebastián, Spain

<sup>2</sup> Department of Physics and Astronomy, University of Bologna, Viale Carlo Berti Pichat 6/2, 40127 Bologna, Italy

<sup>3</sup> Center for Nano Science and Technology@PoliMi, Istituto Italiano di Tecnologia, Via Raffaele Rubattino 81, 20134 Milano, Italy

<sup>4</sup> Politecnico di Milano, Dipartimento di Fisica, Piazza Leonardo da Vinci 32, 20133 Milano, Italy

<sup>5</sup> XMaS/BM28-ESRF, 71 Avenue Des Martyrs, F-38043 Grenoble Cedex, France

Department of Physics, University of Warwick, Gibbet Hill Road, Coventry, CV4 7AL, UK

<sup>6</sup> Department of Chemistry “Giacomo Ciamician”, University of Bologna, 40126 Bologna, Italy

<sup>7</sup> Ikerbasque, Basque Foundation for Science, 48013 Bilbao, Spain

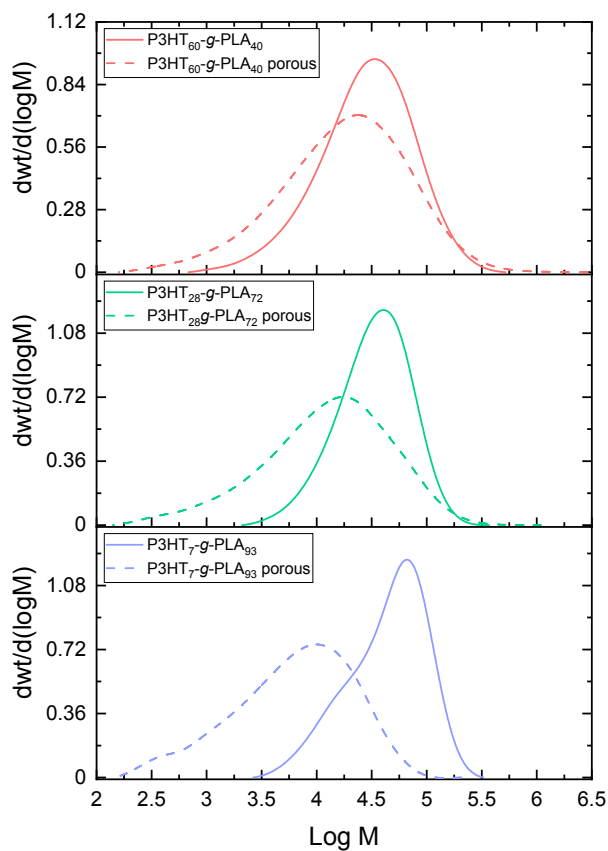


**Figure S1.** Molar mass distribution curves of the synthesized copolymers before after PLA hydrolysis determined by SEC.

**Table S1.** Number-average molecular weight ( $M_n$ ) of the synthesized copolymers after PLA hydrolysis.

Code	Synthesized polymer	$M_n$ (g mol <sup>-1</sup> ) <sup>a</sup>	D <sup>b</sup>
2	P3HT <sub>60</sub> -g-PLA <sub>40</sub> porous	6 300	6.2
3	P3HT <sub>28</sub> -g-PLA <sub>72</sub> porous	4 400	5.9
4	P3HT <sub>7</sub> -g-PLA <sub>93</sub> porous	2 600	4.4

<sup>a</sup> $M_n$  determined by using PS standards; <sup>b</sup>Dispersity (D) =  $M_w/M_n$  calculated by SEC.

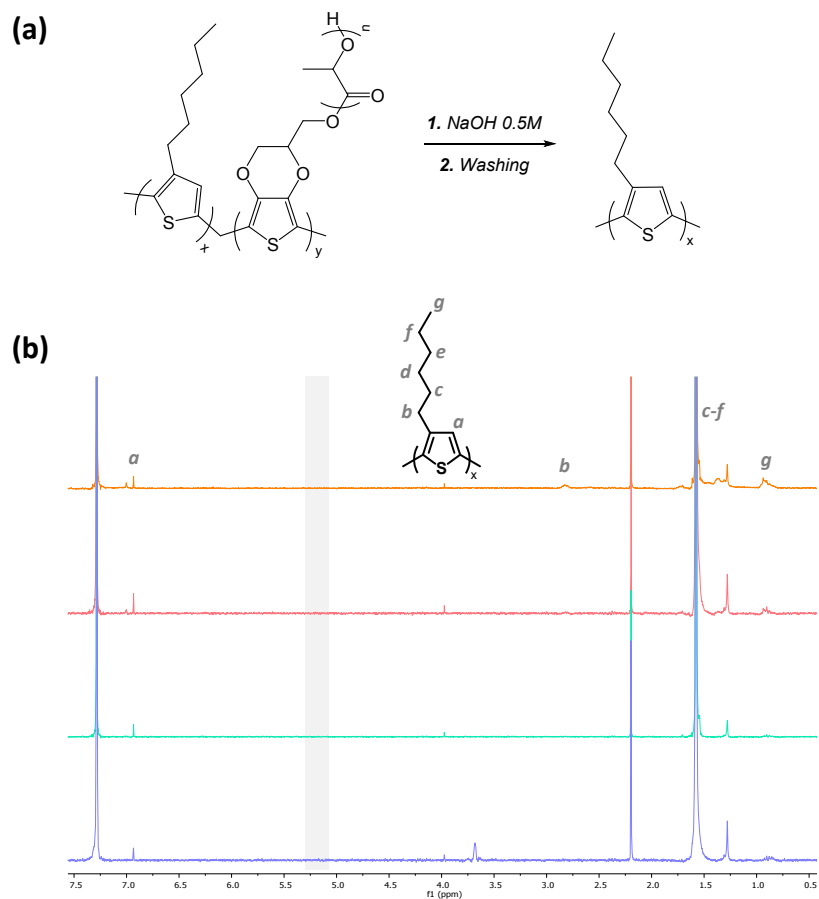


**Figure S2.** (a) Chemical route employed to hydrolyze PLA. (b)  $^1\text{H-NMR}$  spectra of the thin films, P3HT (orange curve), P3HT<sub>60</sub>-g-PLA<sub>40</sub> (red curve), P3HT<sub>28</sub>-g-PLA<sub>72</sub> (green curve), and P3HT<sub>7</sub>-g-PLA<sub>93</sub> (blue curve), after NaOH treatment, to induce the PLA hydrolysis.

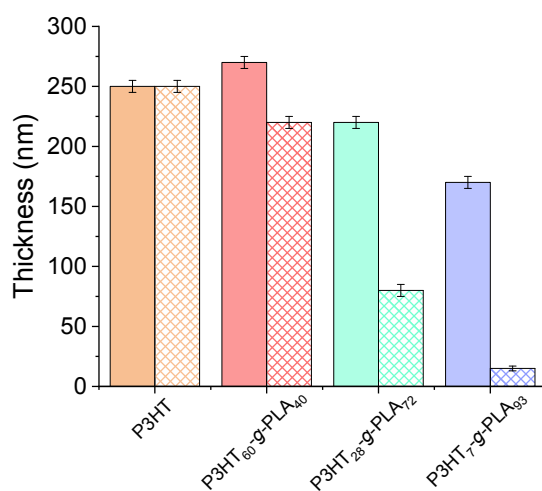


**Figure S3.** Thickness of the non-porous (solid bars) and porous (frame filler bars) films measured by AFM. (b) Water contact angle (WCA) of non-porous (solid bars) and porous (frame filler bars) films.

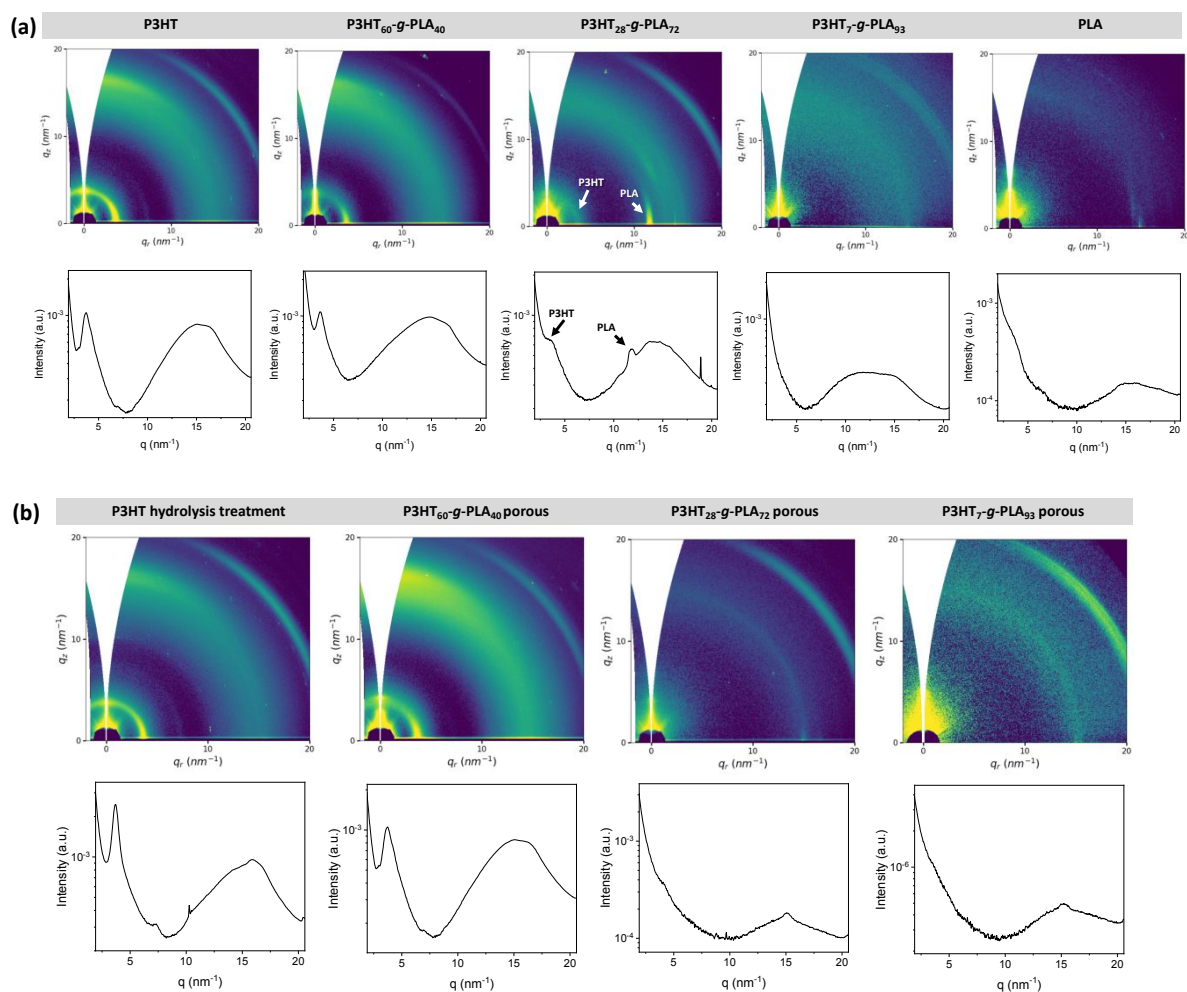


**Figure S4.** 2D GIWAXS images and the corresponding Intensity vs.  $q$  curves plots for the (a) non-porous films made with the homopolymers, P3HT and PLA, and the different graft copolymers P3HT-g-PLA, and (b) porous thin films.

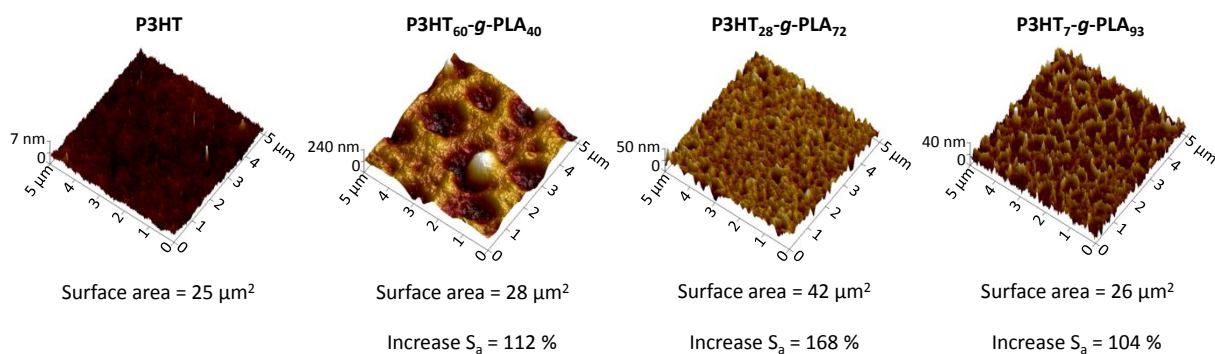


**Figure S5.** 3D AFM height images of porous films and surface area ( $S_a$ ) determined with the software Nanoscope Analysis 1.90 and the Equation 1. The increase  $S_a$  was determined with respect to the surface area of P3HT film.

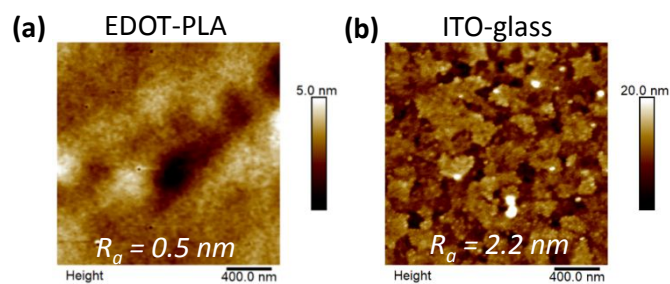


**Figure S6.** Topographical AFM images of the (a) non-porous PLA films and (b) ITO-glass after the complete PLA hydrolysis.

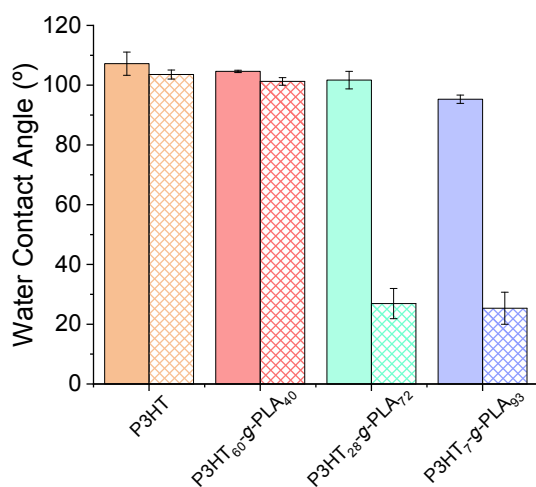


**Figure S7.** Water contact angle (WCA) of non-porous (solid bars) and porous (frame filler bars) films.

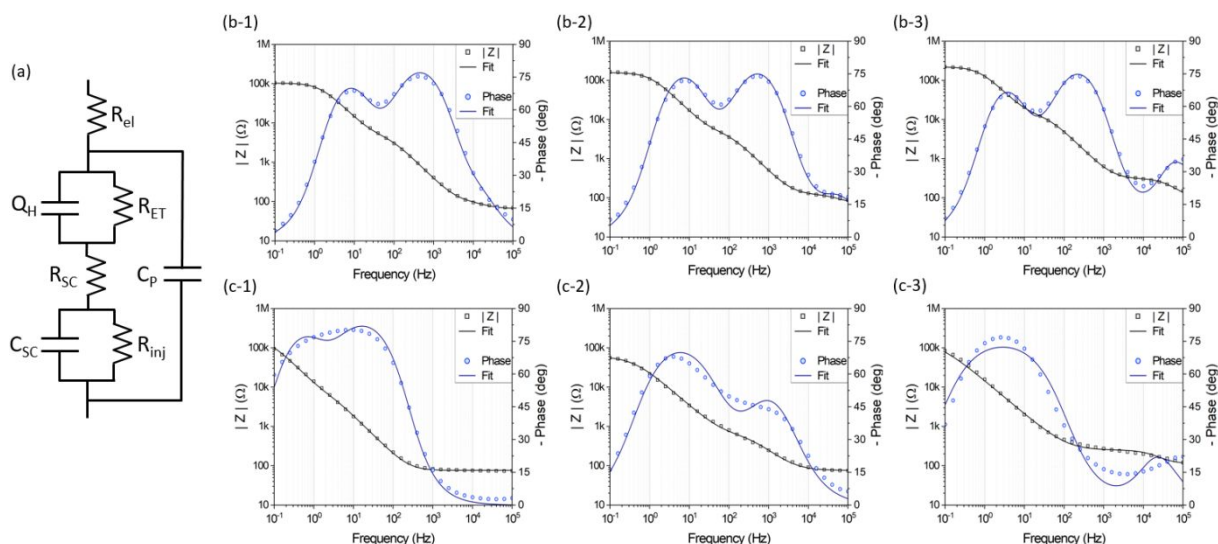


**Figure S8.** (a) Schematic representation of the extended equivalent circuit used to fit the impedance data between 100 mHz and 100 kHz. The circuit includes several elements, namely  $R_{inj}$  and  $C_{SC}$ , representing the injection resistance and the capacitance at the ITO-semiconductor interface,  $R_{SC}$ , the semiconductor resistance that becomes important in thick films,  $Q_H$ , the non-ideal double-layer capacitance which is placed in parallel with the electron transfer resistance  $R_{ET}$  at the interface with water,  $R_{el}$ , the electrolyte resistance, and  $C_p$ , the parallel capacity accounting for the unbalanced charges between ITO and the electrolyte. The impedance curves of the samples and the corresponding fits for non-porous (b) and porous (c) samples are shown as empty symbols and straight lines, respectively. The samples are ordered by thickness: 20 nm (1), 80 nm (2), and 200 nm (3).

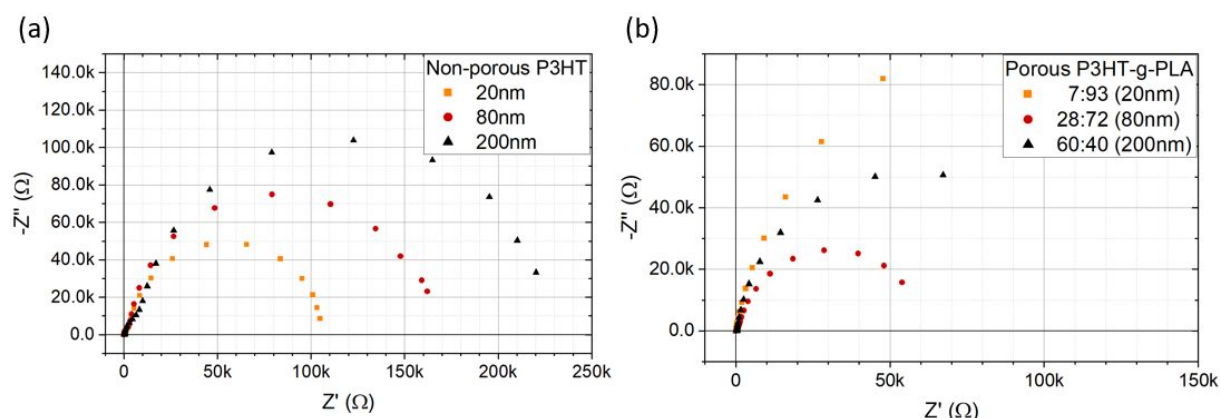


**Figure S9.** Nyquist plots showing impedance data acquired from 100 mHz to 100 kHz for non-porous (a) and porous (b) films.

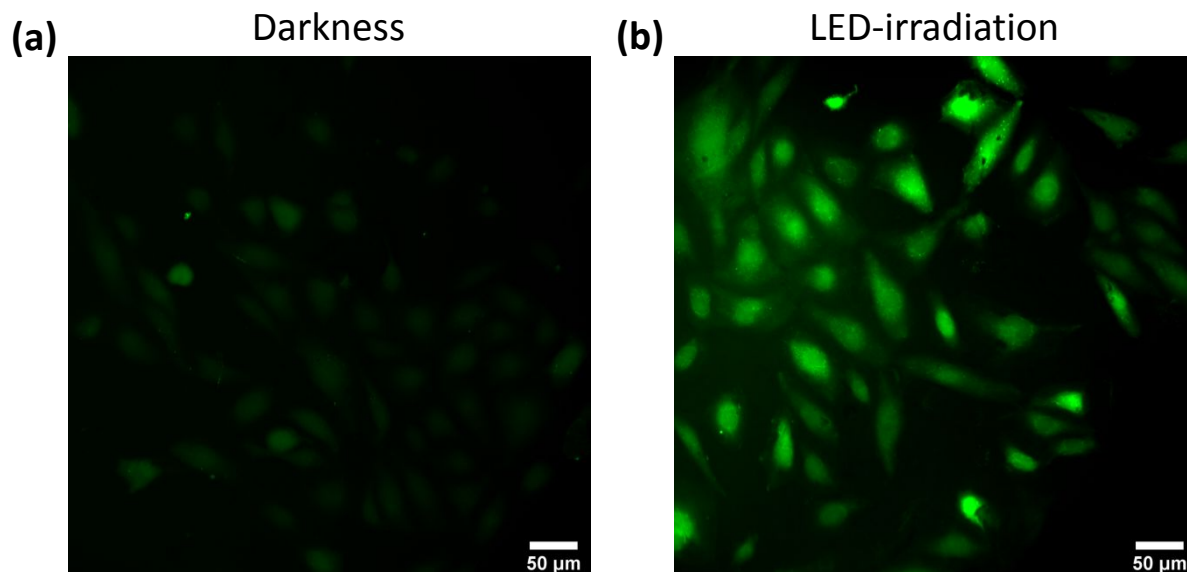


**Figure S10.** Fluorescence images of HUVEC cells cultured on top of the P3HT<sub>28</sub>-g-PLA<sub>72</sub> porous thin films (a) in the darkness and (b) after irradiation with a LED ( $\lambda_{\text{exc}} = 520 \text{ nm}$ ;  $110 \text{ mW cm}^{-2}$ ) for 2.5 s.

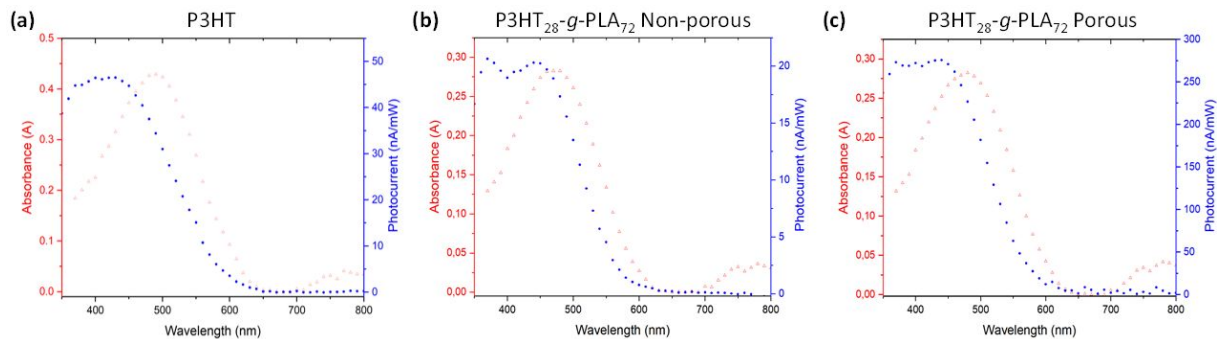


**Figure S11.** Optical absorption and photoelectrochemical current spectra of the three different photoelectrode thin films (a) P3HT, (b) Non-porous P3HT<sub>28</sub>-g-PLA<sub>72</sub>, and (c) Porous P3HT<sub>28</sub>-g-PLA<sub>72</sub> in contact with the electrolyte (PBS at pH 7.4).